# Local structure of liquid and solid silver halides probed by XAFS

**Andrea Di Cicco,[a]* Marco Taglienti,[a] Marco Minicucci[a] and Adriano Filipponi[b]**

[a] INFM, Dip. di Mat. e Fisica, Università di Camerino, Via Madonna delle Carceri, 62032 Camerino (MC), Italy, and [b] INFM, Dipartimento di Fisica, Universita' dell'Aquila, via Vetoio, 67100 Coppito (Aq), Italy. E-mail: dicicco@campus.unicam.it

Investigation of the local structure of the high-temperature liquid and solid phases in the 300-725 K range of AgBr has been performed using the x-ray absorption spectroscopy (XAS). Structural results are compared with existing diffraction studies and computer simulations demonstrating the reliability of the XAS technique in determining the short-range structure. Present results on solid AgBr are in agreement with known thermal expansion data. The short-range $g(r)$ of liquid AgBr is reconstructed showing the unique insight provided by the XAS technique in measuring short-range atom-atom correlations in liquids.

## 1. Introduction

Silver bromide (AgBr) belongs to a class of materials whose bonding character is intermediate between ionic and covalent. Silver halides show different stable structures at ambient pressure depending on the degree of covalent character of the bonding. Silver bromide (AgBr), like silver chloride (AgCl) adopts the rock-salt structure at ambient conditions, while AgI is the less ionic of the class adopting a fourfold coordinated structure (see for example Hull et al., 1999 and ref. therein). In these systems, the ionic conductivity largely increase at high temperature reaching values comparable with that of molten salts before melting. Ionic conductivity and structural properties of these compounds are intimately related and information about local structure is particularly important.

For AgI the onset of superionic conduction is associated with a true first-order phase transition, accompanied by changes in structure and discontinuities of the specific heat. The other silver halides show a continuous increase of the ionic conductivity reaching relatively large values below the melting point. At all temperatures in the solid phase the halogen ions are closely bound to their lattice sites while the cations are more mobile, dominating the ionic conductivity.

In AgBr the rise in the ionic conductivity above a characteristic "knee" temperature of about 370 K is accompanied by an "anomalous" expansion of the lattice. Structural disorder in solid AgBr was investigated using neutron diffraction at high temperature (see Keen et al., 1990, and ref. therein) and XAFS at low temperature (Yokoyama et al., 1989; Batchelor et al., 1995). XAFS results indicated the occurrence of strong anharmonic effects already at 100 K. Important reference papers for XAFS studies on silver and copper halides are those of Hayes et al., 1980 and of Boyce et al., 1981.

The short-range structure of liquid AgBr was studied using RMC (Reverse Monte Carlo) analysis of neutron diffraction data (Keen et al., 1990; Nield et al., 1992) and molecular-dynamics (MD) simulations (Tasseven et al., 1997). Those two structural determination present very different features mainly due to the simple interaction model used for MD calculations. To our knowledge, there is only one Ag $K$-edge XAFS experiment performed on liquid AgBr (Inui et al., 1995). The average local structure determined by XAFS resulted to be incompatible with MD and ND results.

Here, we present some of the structural results obtained by high-quality x-ray absorption measurements of solid and liquid AgBr collected using synchrotron radiation. A complete report of this work will be published elsewhere (Di Cicco et al., 2000). Accurate determination of the local structure is performed using simultaneous Ag and Br $K$-edge XAFS refinement in the framework of the GNXAS method for data-analysis (Filipponi et al., 1995).

## 2. Experimental

The AgBr samples were prepared starting from high-purity powders (99,999%, Aldrich chemicals). The powder was finely ground in a mortar, mixed with graphite and pressed ($P \approx 7 Kbar$) into pellets (thickness $\approx 1 mm$). Samples resulted to be a homogeneous mixture of AgBr isolated micrometric particles into the inert matrix (graphite) as verified by optical microscopy.

Samples were characterized by x-ray diffraction as a function of temperature using a Mo rotating anode source and a high-temperature furnace of original design on a powder diffractometer (Centro Interdipartimentale Grandi Apparecchiature, Università di Camerino). The thermal expansion of AgBr grains was found to be in agreement with previous measurements (Lawn, 1963). Pellets were stored under inert atmosphere and protected from light before performing x-ray absorption measurements.

The Br $K$-edge and Ag $K$-edge XAFS spectra were measured in transmission mode on beamline BM29 at the European Synchrotron Radiation Facility (ESRF, Grenoble), equipped with a fixed-exit Si (311) double-crystal monochromator achieving a resolving power of about $10^4$ with 0.4 mm aperture for the primary slits. XAFS measurements were collected using ionization chambers in a wide range of temperature 30-927 K in the solid and liquid phases. Low-temperature measurements were performed using a closed-cycle He cryostat available on the beamline, while high-temperature experiments were realized using an improved version of a previously described XAFS furnace (Filipponi et al., 1994).

At temperatures higher than 1000 K the sample starts to evaporate, as we have observed looking at the modification of the absorption discontinuity. Measurements were performed verifying that at a given temperature the absorption discontinuities at the Br and Ag $K$-edges remained constant within the errors over several successive scans. The signal-to-noise ratio resulted to be excellent, better than $10^4$, in all cases including Br $K$-edge spectra. In such conditions, even low-amplitude oscillations such as those typical of the liquid phase can be reliably analyzed.

## 3. Solid AgBr

AgBr XAFS data collected at both $K$ edges in the 300-670 K temperature range are shown in Fig. 1. Raw data are compared with the results of the simultaneous refinement of the Br and Ag $K$-edge XAFS $k\chi(k)$ data of solid AgBr (barely visible on that scale).

Data-analysis of raw Br $K$-edge and Ag $K$-edge XAFS data was carried out by minimizing a $\chi^2$-like residual function in the space of structural and background parameters following the multi-edge method discussed in previous publications (Di Cicco, 1996). Present double-edge fitting was performed taking account of the well-known multi-electron channels occurring in the background of Br and Ag $K$-edge XAFS spectra (see for example Li et al. *et*

al., 1992; D'Angelo *et al.* 1993; Gomilšek *et al.* 1999, Filipponi 1995, Filipponi *et al.* 1995) which can interfere with the structural XAFS oscillations.

The structural $\chi(k)$ XAFS signal has been calculated taking into account the two-body and three-body configurations of solid AgBr up to the fourth coordination shell and using the irreducible multiple-scattering $\gamma^{(n)}$ signal decomposition (Filipponi *et al.* 1995). The agreement between experimental and best-fit theoretical signals is excellent for both edges.
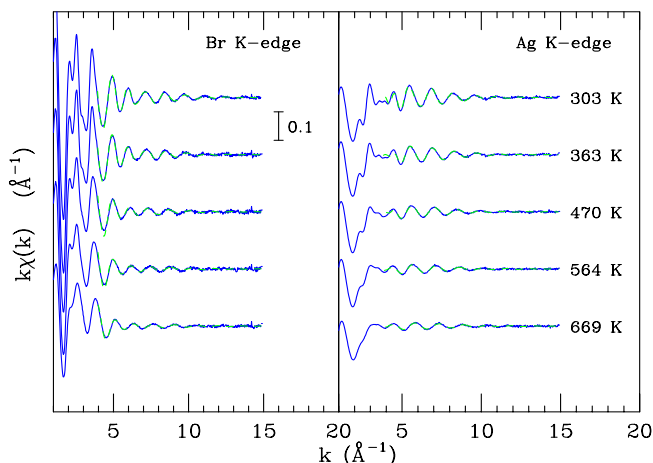


**Figure 1**
Experimental and best-fit (dash) calculated XAFS $k\chi(k)$ spectra of solid AgBr for increasing temperature (from the top to the bottom). The agreement is excellent at all temperatures.

The dominant contribution to the total XAFS signal is given by the first-neighbor two-body signal $\gamma_1^{(2)}$. This situation occurs at all temperatures, although at low temperatures the two-body and higher-order signals associated with farther atoms become gradually more important. The best-fit curves (dash) compared with the raw data in Fig. 1 have been calculated using the whole set of structural and non-structural parameters related to four coordination shells. However, only the first-neighbor structural parameters $R$ (average distance), $\sigma^2$ (distance variance) and $\beta$ (skewness) can be accurately refined, due to the weak amplitude of the multiple-scattering signals associated with the remaining structural parameters. It should be noted that those signals are indeed dependent on the first-neighbor distribution, although they obviously contain information about three-body correlations. Therefore they are useful for obtaining a more accurate determination of the first-neighbor distribution. Structural results concerning the first-neighbor distribution in solid AgBr, obtained using this approach in a large temperature interval, are contained in Table 1, where we report the three parameters defining the first-neighbor distribution $R$, $\sigma^2$, and $\beta$. The third cumulant of the distribution, obtained as $K_3 = \beta\sigma^3$, is also reported.

**Table 1**
Structural parameters for the first-neighbor distribution in solid AgBr. The statistical error bar is indicated in brackets.

| T (K) | $R$(Å) | $\sigma^2$(Å$^2$) | $\beta$ | $K_3$ (Å$^3$) |
|-------|--------|-------------------|---------|---------------|
| 303 | 2.893(2) | 0.0285(4) | 0.67(2) | $32(3)\times10^{-4}$ |
| 363 | 2.902(3) | 0.034(1) | 0.70(3) | $44(4)\times10^{-4}$ |
| 470 | 2.918(4) | 0.048(2) | 0.80(4) | $85(7)\times10^{-4}$ |
| 564 | 2.943(6) | 0.065(2) | 0.91(4) | $15(1)\times10^{-3}$ |
| 669 | 2.992(7) | 0.102(3) | 1.05(5) | $34(3)\times10^{-3}$ |

Present results are in agreement with thermal expansion data obtained by x-ray diffraction and do not show the apparent contraction of distances found in previous XAFS studies at low temperatures (Yokoyama *et al.*, 1989; Batchelor *et al.*, 1995). This result, incompatible with known thermal expansion data (Lawn, 1962), was probably obtained because anharmonic effects were not properly accounted for. Present agreement with diffraction data indicates that the Γ-like model (Filipponi *et al.*, 1995; Di Cicco *et al.* 1996; Minicucci *et al.* 1997) is sufficiently accurate in describing deviations from the harmonic approximation in this ionic system.

## 4. Liquid AgBr

The model pair distribution functions obtained using MD simulations (Tasseven *et al.*, 1997) and ND-RMC experiments (Keen *et al.*, 1990) were used to calculate the corresponding Br and Ag $K$-edge $\gamma^{(2)}$ XAFS structural signals through direct integration over the $g(r)$'s (Filipponi, 1994; Di Cicco 1996; Di Cicco *et al.* 1997)

From the comparison shown in Fig. 2 it is evident that both models are unable to account for the observed XAFS signal. For the MD model (lower panels), which generates a signal dominated by the Ag-Br partial, the difference in phase indicates that the Ag-Br effective distance measured by XAFS is longer than in the MD simulation. The larger amplitude of the experimental signal indicates that the rise of the first-neighbor peak is steeper than expected looking at MD calculations. In the case of the RMC-ND model (upper panels) the $g_{AgBr}$ partial generates a $\gamma^{(2)}$ signal with a phase in better agreement with the experimental XAFS data, but still too weak. For this model the $g_{BrBr}$ partial generates a strong high-frequency signal which is not observed in the experimental XAFS spectra. Similarly the model predicts a non negligible signal from the $g_{AgAg}$ partial. This signal contains high frequency components which are an artifact from some sharp features and a low frequency component that may be present in the experimental data.
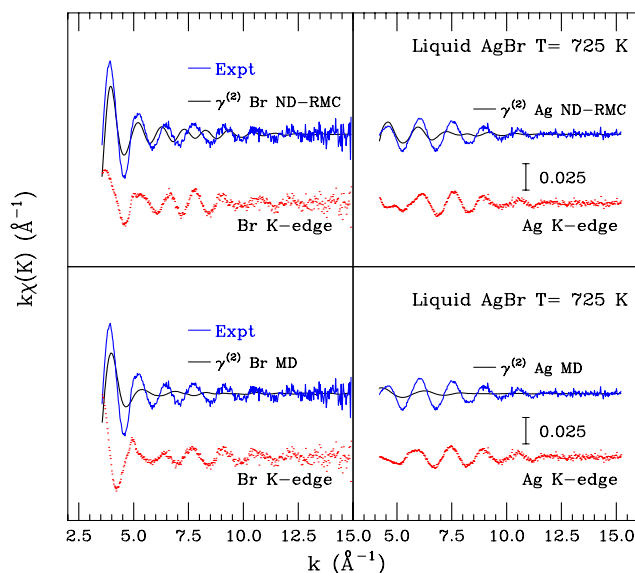


**Figure 2**
Upper panels: Br (left) and Ag (right) $K$-edge XAFS $k\chi(k)$ experimental data (Expt) of liquid AgBr compared with the total $k\gamma^{(2)}(k)$ signal derived from reverse Monte-Carlo analysis of Residual spectra for each edge are the lowermost curves. Lower panels: Br (left) and Ag (right) $K$-edge XAFS $k\chi(k)$ experimental data (Expt) of liquid AgBr compared with the total $k\gamma^{(2)}(k)$ signal derived from molecular-dynamics calculations (MD). Residual spectra for each edge are the lowermost curves.

The comparison of the calculated and experimental XAFS spectra indicates that a structural refinement is necessary to improve the agreement with the experimental data. The short-range refinement of the pair distribution function has been performed using the procedure described in previous publications (Filipponi, 1994; Di Cicco *et al.*, 1997; Minicucci *et al.*, 1997). The starting model $g(r)$'s are decomposed in the sum of short range peaks plus long-range tails. The total signal is calculated by adding all these contributions, but only that from the short range peaks is fitted to the experimental data. Constraints on the structural parameters are introduced to satisfy long-range order properties of the structure. The constraints originally derived for mono-atomic systems (Filipponi, 1994) can be extended also to the two-component ionic liquid under consideration, because the $q \rightarrow 0$ limit of the partial structure factors is $\rho k_B T K_T$ where $K_T$ is the isothermal compressibility (March and Tosi, 1991).

Details of the decomposition method used for ionic binary melts can be found in Di Cicco *et al.*, 1997 and Minicucci *et al.*, 1997. Both MD and ND-RMC models were put to a test for structural refinement and the first one (MD) was observed to give the more accurate refinement. In Fig. 3 (left) we report the best-fit results for liquid AgBr at T = 725 K using the MD simulation results as starting structural model. The short-range $\gamma^{(2)}$ AgBr signals dominate the whole Ag $K$-edge XAFS spectra of the liquid and the final best-fit calculated curve results to be in very good agreement with the experimental data.

The reconstructed $g_{AgBr}$ short-range distribution functions is compared in Fig. 3 (right) with the MD and ND-RMC models.
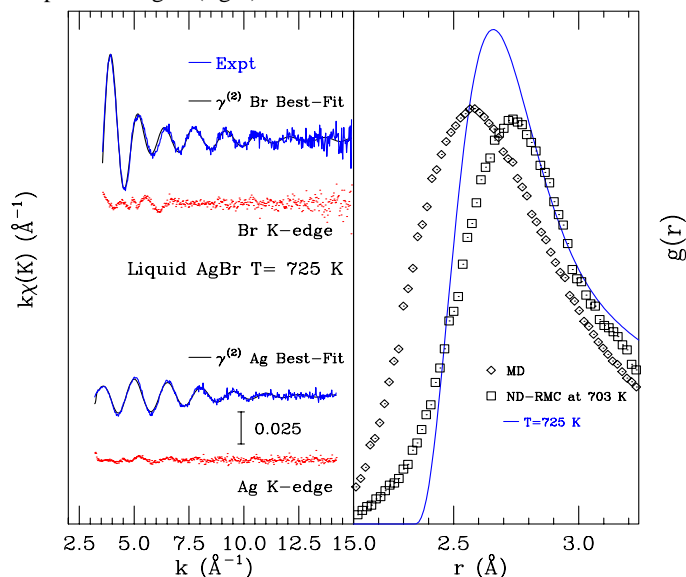


**Figure 3**

Left panel: Br (upper part) and Ag (lower part) $K$-edge XAFS $k\chi(k)$ experimental data (Expt) of liquid AgBr at $T = 725$ K compared with the best-fit $k\gamma^{(2)}(k)$ signal obtained refining the shape of the short-range $g_{AgBr}$ peak. The agreement between calculated and experimental spectra is excellent. Right panel: Comparison between previous $g_{AgBr}(r)$ determinations by neutron diffraction (ND-RMC), molecular-dynamics simulations (MD), and present XAFS refinement as a function of temperature.

The new determination shows that a much steeper rise of the first peak of the partial distribution. This feature is absolutely necessary to reproduce the intensity of the XAFS oscillations at both edges. The MD simulation results to be shifted toward shorter distances, suggesting that improvements in the model interionic potentials are necessary to obtain realistic structural results. The ND-RMC determination shows a tail on the short-distance side which is not compatible with XAFS experimental results. Looking at Fig. 3 we observe that the $g_{AgBr}$ peak is shifted toward shorter distances, decreasing its height upon increasing the temperature. The peak turns out to be broadened at higher temperature but the distance of closest approach is reduced of about .03 Å due to the effect of the repulsive interaction. The peak becomes more asymmetric and broadened toward the longer distances side. The $g(r)$ reconstructed by XAS can be useful to devise new interaction models in ionic liquids.

## References

D. R. Batchelor, P. Tangyunyong, T. N. Rhodin, Y. T. Tan, and K. J. Lushington, Sol. St. Comm. **94**, 179 (1995).

J. B. Boyce, T. M. Hayes, and J. C. Mikkelsen, Jr., Phys. Rev. B **23**, 2876 (1981).

P. D'Angelo, A. Di Cicco, A. Filipponi, N. V. Pavel, Phys. Rev. A **47**, 2055 (1993).

A. Di Cicco, M. J. Rosolen, R. Marassi, R. Tossici, A. Filipponi, and J. Rybicki, J. Phys.: Condens. Matter **8**, 10779 (1996).

A. Di Cicco, Phys. Rev. B **53**, 6174 (1996).; A. Di Cicco, J. de Physique IV Colloque C2, 171 (1997).

A. Di Cicco, M. Minicucci, and A. Filipponi, Phys. Rev. Lett. **78**, 460 (1997).

A. Di Cicco, M. Taglienti, M. Minicucci, and A. Filipponi, to be published in Phys. Rev. B (2000).

A. Filipponi, J. Phys.: Condens. Matter **6**, 8415 (1994).

A. Filipponi and A. Di Cicco, Nucl. Instr. & Methods for Phys. Res. B **93**, 302 (1994).

A. Filipponi, Physica B **208&209**, 29 (1995).

A. Filipponi and A. Di Cicco, Phys. Rev. A **52**, 1072 (1995).

A. Filipponi, A. Di Cicco, and C. R. Natoli, Phys. Rev. B **52**, 15122 (1995).

A. Filipponi and A. Di Cicco, Phys. Rev. B **51**, 12322 (1995).

T. M. Hayes and J. B. Boyce, J. Phys. C: Solid State Phys. **13**, L731 (1980).

S. Hull and D. A. Keen, Phys. Rev. B **59**, 750 (1999).

M. Inui, S. Takeda, K. Maruyama, Y. Shirakawa, and S. Tamaki, J. Non-Cryst. Sol. **192& 193**, 351 (1995).

D. A. Keen, W. Hayes, R. L. McGreevy, J. Phys.: Condens. Matter **2**, 2773 (1990).

B. R. Lawn, Acta Cryst. **16**, 1163 (1963).

G. Li, F. Bridges, and G. S. Brown, Phys. Rev. Lett. **68**, 1609 (1992).

N. H. March and M. P. Tosi, *Atomic Dynamics in Liquids* (Dover, New York, 1991).

M. Minicucci and A. Di Cicco, Phys. Rev. B **56**, 11456 (1997).

V. M. Nield, D. A . Keen, W. Hayes, and R. L. McGreevy, J. Phys.: Condens. Matter **4**, 6703 (1992).

V. M. Nield, R. L. McGreevy, D. A . Keen, and W. Hayes, Physica B **202**, 159 (1994).

J. Padežnik Gomilšek, A. Kodre, I. Arčon, A. M. Loireau-Lozac'h, and S. Bénazeth, Phys. Rev. A **59**, 3078 (1999).

Ç. Tasseven, J. Trullàs, O. Alcaraz, M. Silbert, and A. Giró, J. Chem. Phys. **106**, 7286 (1997).

T. Yokoyama, T. Satsukawa, and T. Ohta, Jap. J. Appl. Phys. **10**, 1905 (1989).